

# Liquid-to-liquid phase transition in pancake vortex systems

Joonhyun Yeo

*Department of Physics, Konkuk University, Seoul, 143-701 Korea*

M. A. Moore

*Department of Physics, University of Manchester, Manchester M13 9PL, United Kingdom*

(October 29, 2018)

We study the thermodynamics of a model of pancake vortices in layered superconductors. The model is based on the effective pair potential for the pancake vortices derived from the London approximation of a version of the Lawrence-Doniach model which is valid for extreme type-II superconductors. Using the hypernetted-chain (HNC) approximation, we find that there is a temperature below which multiple solutions to the HNC equations exist. By explicitly evaluating the free energy for each solution we find that the system undergoes a first-order transition between two vortex liquid phases. The low-temperature phase has larger correlations along the field direction than the high-temperature phase. We discuss the possible relation of this phase transition to the liquid-to-liquid phase transition recently observed in Y-Ba-Cu-O superconductors in high magnetic fields in the presence of disorder.

## I. INTRODUCTION

The properties of flux lines in high temperature superconductors in a magnetic field have been under theoretical and experimental investigation for many years but surprises continue to appear. The first-order transition line observed in experiments [1–4] well below the upper critical field  $H_{c2}(T)$  is usually interpreted as a melting line of a vortex lattice into a vortex liquid. For Y-Ba-Cu-O (YBCO) superconductors, the first-order nature of the transition disappears at critical points in both high [1,2] and low [3,4] magnetic fields. Unlike the upper critical point, which is usually attributed to the effect of disorder, the value of the lower critical field seems to be determined by the oxygen content of the sample [4]. In Ref. [5] a different interpretation of the first order transition was given in terms of a transition between two liquid phases with different correlation lengths along the magnetic field direction. The disappearance of the first-order transition line at low magnetic fields is explained naturally as a critical end-point in this picture. For fields higher than the upper critical point, the effect of disorder is increasingly important. In a recent experiment on YBCO [2], a rich phase diagram at fields above the upper critical field was revealed, which included two liquid phases separated by a second-order (continuous) transition. Although this transition appears in the regime where the effect of disorder is large, it is a reversible thermodynamic phase transition the nature of which is yet to be understood theoretically. We believe that the results of this paper will be a step towards the understanding of this liquid-to-liquid transition.

In Section II we shall introduce a model for the vortex system in a layered superconductor in a magnetic field perpendicular to the layers. We focus for simplicity

only on the case where the effect of disorder is negligible. The model is based on the London approximation of the Lawrence-Doniach model and consists of a system of pancake vortices in each layer interacting via an effective pair potential obtained by integrating out the degrees of freedom other than those of the pancake vortices. We find that the present model exhibits a first-order transition between two liquid phases with very different correlations along the field direction. The state below the transition is very strongly correlated along the field direction such that the pancake vortices are likely to be stacked on top of each other rather as if in a stiff vortex line, while above the transition in the high temperature phase the vortex line is dissociated resulting in a phase with very short correlation lengths.

We note that our liquid-to-liquid transition differs from another phase transition between two vortex liquid phases, namely the disentanglement transition, that has been studied and debated for some time [6]. In the present model, unlike below the disentanglement transition, there is no long range order along the field direction. On the other hand, it might be possible to associate the present liquid-to-liquid transition with the one observed in the recent experiment [2] on YBCO at fields above the upper critical point. Since the effect of disorder has not been considered in this model, it is impossible to make a quantitative comparison of the present result with the experimental results in Ref. [2]. Also the orders of the phase transition are different from each other. We observe, however, that a first order phase transition in the absence of disorder becomes a continuous transition when the disorder exceeds a critical amount [7]. This will also be the case in our model. It is our contention that the basic mechanism that drives the liquid-to-liquid phase transition in our model is also responsible for the transi-

tion observed in Ref. [2].

In this paper the hypernetted chain (HNC) approximation is used to calculate thermodynamic quantities and correlation functions. The HNC approximation is often used for describing correlations in classical liquids [8]. We set up and solve numerically the HNC integral equations corresponding to the pair potential for the pancake vortex system. The first order transition emerges when below a certain temperature the HNC equations admit *multiple* solutions. By calculating and comparing the free energy of these solutions we can determine the thermodynamically stable branch of solutions. We believe it is quite rare in the HNC analysis of classical liquids to find multiple solutions and first order transitions in this way. Calculations on vortex liquids based on the HNC approximation have also been done in Ref. [9], but using a pair potential which does *not* include the Josephson coupling between the layers as done here. The authors of Ref. [9] used only a phenomenological melting criterion without considering the possibility of multiple solutions to their HNC equations.

The paper is organized as follows. In the next section we introduce the model, derive the pair potential for the pancake vortices, and set up the HNC equations. The results based on the numerical solution to the HNC equations are presented and discussed in Section III.

## II. MODEL

### A. Derivation of the pair potential

Our starting point is the Lawrence-Doniach (LD) model [10] for a layered superconductor in a magnetic field along the  $c$ -axis perpendicular to the layers. With the order parameter in the  $n$ -th layer denoted by  $\psi_n$ , the LD Hamiltonian is given by

$$\begin{aligned}
H[\psi, \psi^*] = & \sum_n d_0 \int d^2\mathbf{r} \left[ \alpha |\psi_n(\mathbf{r})|^2 + \frac{\beta}{2} |\psi_n(\mathbf{r})|^4 \right. \\
& + \frac{1}{2m_{ab}} \left| (-i\hbar\nabla - \frac{e^*}{c}\mathbf{A})\psi_n \right|^2 \\
& \left. + \frac{\hbar^2}{2m_c d^2} |\psi_n(\mathbf{r}) - \psi_{n+1}(\mathbf{r})|^2 \right], \quad (1)
\end{aligned}$$

where  $d_0$  is the layer thickness,  $d$  the layer spacing and  $\alpha$ ,  $\beta$ ,  $m_{ab}$ , and  $m_c$  phenomenological parameters.

In the London approximation the magnitude  $|\psi_n|$  of the order parameter  $\psi_n(\mathbf{r}) = |\psi_n| \exp(i\phi_n(\mathbf{r}))$  is held fixed and the fluctuations of only the phase  $\phi_n(\mathbf{r})$  is considered. We consider the extreme type-II case where the magnetic field  $\mathbf{B} = \nabla \times \mathbf{A}$  is constant and uniform. The Hamiltonian becomes after neglecting constant terms

$$\mathcal{H} = \sum_n \int d^2\mathbf{r} \left[ \frac{J}{2} (\nabla\phi_n - \mathbf{a})^2 + \frac{J}{2\gamma^2 d^2} (\phi_{n+1} - \phi_n)^2 \right], \quad (2)$$

where  $J = \hbar^2 |\psi|^2 d_0 / m_{ab}$ ,  $\mathbf{a} = (2\pi/\Phi_0)\mathbf{A}$  with  $\Phi_0 = hc/2e$ , and  $\gamma = (m_c/m_{ab})^{1/2}$  is the anisotropy parameter. In the above equation we approximated the inter-layer Josephson coupling term as  $2(1 - \cos(\phi_{n+1} - \phi_n)) \simeq (\phi_{n+1} - \phi_n)^2$ . It is convenient to introduce two dimensionless parameters to specify the system. They are  $\Gamma \equiv 2\pi\beta J$  and  $\eta \equiv (a/\gamma d)^2$  where  $\beta = 1/k_B T$  is the inverse temperature and  $a = (\pi\sigma)^{-1/2}$  is the inter-pancake vortex spacing with  $\sigma$  being the number density of the pancake vortices for each layer that is in turn determined by the magnetic field  $B$ . In terms of the physical parameters, they are given by

$$\Gamma = \frac{2}{k_B T} \left( \frac{\Phi_0}{4\pi\lambda} \right)^2, \quad \eta = \frac{1}{\pi\gamma^2 d^2} \left( \frac{\Phi_0}{B} \right), \quad (3)$$

where  $\lambda$  is the penetration depth parallel to the layers. High temperatures thus correspond to small values of  $\Gamma$ , low temperatures to high values of  $\Gamma$ , and  $\eta$  is a measure of the coupling between layers.

In order to focus on the vortex degrees of freedom, we decompose the phase variable  $\phi_n$  into the ‘‘spin-wave part’’  $\varphi_n$  and the vortex part  $\Theta_n$  for each layer,  $\phi_n = \varphi_n + \Theta_n$ , and integrate out the spin-wave part. To do this it is convenient to introduce the Fourier transform:

$$\varphi_n(\mathbf{r}) = \frac{1}{dN_l} \sum_q \int \frac{d^2\mathbf{k}}{(2\pi)^2} \tilde{\varphi}_q(\mathbf{k}) \exp(iqnd + i\mathbf{k} \cdot \mathbf{r}).$$

In this paper we consider a system which consists of a stack of  $N_l$  layers, on which we impose periodic boundary conditions in the direction perpendicular to the layers;  $\varphi_{n+N_l}(\mathbf{r}) = \varphi_n(\mathbf{r})$ . where  $q = 2\pi j/N_l d$  and we use  $N_l$  integer values of  $j$  in the sum such that the wavevector  $q \in [-\pi/d, \pi/d]$  belongs to the first Brillouin zone.  $\tilde{\Theta}_q(\mathbf{k})$  is defined in the same way. For future use we introduce the hatted quantity  $\hat{\varphi}_n \equiv (\sigma/d)\tilde{\varphi}_n$  for each function. It is straightforward to integrate over  $\varphi_q$  to obtain the vortex part of the Hamiltonian given by

$$\begin{aligned}
\mathcal{H}_V = & \frac{J}{2} \left[ \int d^2\mathbf{r} \sum_n (\nabla\Theta_n - \mathbf{a})^2 + \frac{1}{dN_l} \sum_q \right. \\
& \left. \times \int \frac{d^2\mathbf{k}}{(2\pi)^2} \frac{\frac{2\eta}{a^2}(1 - \cos qd)}{k^2 + \frac{2\eta}{a^2}(1 - \cos qd)} k^2 \tilde{\Theta}_{-q}(-\mathbf{k}) \tilde{\Theta}_q(\mathbf{k}) \right]. \quad (4)
\end{aligned}$$

The above Hamiltonian represents pancake vortices on each layer interacting through some pair potential  $v_n(\mathbf{r})$  which can be read off from the above equation as follows. The key point in deriving the pair potential for the pancake vortices is to note that one can write the pancake vortex density  $\rho_n(\mathbf{r}) = \sum_i \delta^{(2)}(\mathbf{r}_n - \mathbf{r}_n^{(i)})$  as

$$\rho_n(\mathbf{r}) = \left| \frac{1}{2\pi} \nabla \times \nabla\Theta_n(\mathbf{r}) \right| = \frac{1}{2\pi} \nabla^2 \Theta_n'(\mathbf{r}),$$

where  $\Theta'_n(\mathbf{r})$  is given by  $\partial_x \Theta_n = -\partial_y \Theta'_n$ ,  $\partial_y \Theta_n = \partial_x \Theta'_n$ . In the above expression  $\mathbf{r}_n^{(i)}$  are the positions of the pancake vortices. We also note that  $(\nabla \Theta_n)^2 = (\nabla \Theta'_n)^2$  and  $-k^2 \widetilde{\Theta}'_q(\mathbf{k}) = \widetilde{\rho}_q(\mathbf{k})$ . Finally to get the pair potential  $v_n(\mathbf{r})$ , we write the Hamiltonian in terms of  $\rho_n$  as follows:

$$\mathcal{H}_V = \frac{1}{2} \sum_{n,n'} \int d^2 \mathbf{r} d^2 \mathbf{r}' \rho_n(\mathbf{r}) v_{n-n'}(\mathbf{r} - \mathbf{r}') \rho_{n'}(\mathbf{r}').$$

For the case where there is no inter-layer coupling,  $\eta = 0$ , we can see using the above procedure that the pair potential behaves as  $1/k^2$ , *i.e.* logarithmically in real space and that  $\mathcal{H}_V$  describes  $N_l$  independent copies of the two-dimensional one-component plasma (OCP) where charged particles interact with each other via a potential which is the logarithm of their spatial separation, all in the presence of a neutralizing background charge. The long-ranged nature of the interaction is a direct consequence of neglecting the screening of the magnetic field. The neutralizing background is provided here by the applied field represented by  $\mathbf{a}$ . In the presence of the inter-layer coupling we can generalize this analysis and we find that the pair potential,  $\widehat{w}_q(\mathbf{k}) \equiv \beta \widehat{v}_q(\mathbf{k})$  is given by

$$\widehat{w}_q(\mathbf{k}) = k_D^2 \left[ \frac{2}{k^2} - \frac{1}{k^2 + \frac{2\eta}{a^2}(1 - \cos qd)} \right], \quad (5)$$

where  $k_D^2 = 2\pi\sigma\Gamma$ . In real space, the potential energy between two pancakes in the same layer is logarithmic and repulsive: between pancakes in different layers there is an attractive Coulomb-like interaction. It is this attractive interaction which is the origin of the liquid-liquid transition and a low-temperature phase where a pancake tends to stack on top of one in the layer below to form a stiff vortex line in order to take advantage of the forces of attraction between them.

## B. HNC equations

We shall set up and solve the HNC equations associated with the pair potential (5). First the direct correlation function  $c_n(\mathbf{r})$  and the pair correlation function  $h_n(\mathbf{r})$  are related through the Ornstein-Zernike relation,

$$\widehat{h}_q(\mathbf{k}) = \frac{\widehat{c}_q(\mathbf{k})}{1 - \widehat{c}_q(\mathbf{k})}. \quad (6)$$

The pair distribution function  $g_n(\mathbf{r}) = h_n(\mathbf{r}) + 1$  is given in terms of the other correlation functions via the HNC closure equation [8],

$$g_n(\mathbf{r}) = \exp[-\beta v_n(\mathbf{r}) - c_n(\mathbf{r}) + h_n(\mathbf{r})]. \quad (7)$$

In the following we shall solve these equations numerically. It is well known from the previous studies

[11] of the two-dimensional OCP using the HNC approximation, one should take special care of the long-ranged logarithmic potential. In the present model the long-range tails in the pair potential are given by the terms singular as  $1/k^2$  for small  $k$  in  $\widehat{w}_q(\mathbf{k})$ . These tails behave as  $(2 - \delta_{q,0})k_D^2/k^2$ . We separate the pair potential into the short-range part with an arbitrary momentum cutoff  $Q$  and the remaining long-range part:  $\widehat{w}_q(\mathbf{k}) = \widehat{w}_q^{(s)}(\mathbf{k}) + \widehat{w}_q^{(l)}(\mathbf{k})$ , where

$$\widehat{w}_q^{(s)}(\mathbf{k}) = (2 - \delta_{q,0}) \frac{k_D^2}{k^2 + Q^2} - (1 - \delta_{q,0}) \frac{k_D^2}{k^2 + \frac{2\eta}{a^2}(1 - \cos(qd))}, \quad (8)$$

$$\widehat{w}_q^{(l)}(\mathbf{k}) = (2 - \delta_{q,0}) \frac{k_D^2 Q^2}{k^2(k^2 + Q^2)}. \quad (9)$$

According to Eq. (7), the long-range part of the pair potential must be cancelled by a long-range part of the direct correlation function, *i.e.*  $c_n(\mathbf{r}) = c_n^{(s)}(\mathbf{r}) + c_n^{(l)}(\mathbf{r})$  where  $c_n^{(l)}(\mathbf{r}) = -w_n^{(l)}(\mathbf{r})$  such that Eq. (7) only involves short-range functions:

$$g_n(\mathbf{r}) = \exp[-w_n^{(s)}(\mathbf{r}) - c_n^{(s)}(\mathbf{r}) + h_n(\mathbf{r})]. \quad (10)$$

Eqs. (6) and (10) form a closed set which we solve iteratively. There are many equivalent iteration methods. Here we start from some function  $c_n^{(s)}(\mathbf{r})$  and calculate  $\widehat{N}_n^{(s)}(\mathbf{k}) \equiv \widehat{h}_n(\mathbf{k}) - \widehat{c}_n^{(s)}(\mathbf{k})$  from Eq. (6). Then we obtain the updated  $c_n^{(s)}(\mathbf{r})$  from Eq. (10) and the definition  $N_n^{(s)}(\mathbf{r})$ . In the numerical calculation it is crucial to have rapid convergence. Here we employ the method introduced in Ref. [12], where a combination of several previous steps were used as an updated  $c_n^{(s)}(\mathbf{r})$ . We utilize the results from the *five* previous iterations to produce a new input function. For small values of  $\Gamma$  it is sufficient to start from  $c_n^{(s)}(\mathbf{r}) = 0$  as the initial function. We then solve the HNC equations for fixed  $\eta$  and for increasing values of  $\Gamma$  using the solution obtained for lower values of  $\Gamma$ .

## III. RESULTS AND DISCUSSION

In this section we present the numerical solutions to the HNC equations described above. Our calculation is done mainly on a system consisting of  $N_l = 11$  layers. In the last part of the section we consider how the solutions behave for larger values of  $N_l$ .

One of the most important results of the present work is that the HNC equations describing a pancake vortex liquid admit multiple solutions over a range of values of  $\eta$  and  $\Gamma$ . This arises in the numerical calculation in the following manner. We find that the solutions which are obtained in the way described above cease to exist

above some value  $\Gamma_I$ . We call these solutions type-I. For  $\Gamma$  smaller than  $\Gamma_I$  we were able to find another type of solutions (type II) which are different from the type-I solutions but which approaches the type-I solution as  $\Gamma \rightarrow \Gamma_I$ . The type-II solutions continue to exist as long as  $\Gamma \geq \Gamma_{II}$  for some  $\Gamma_{II}$ . Below  $\Gamma_{II}$  again the type-II solution disappears. We then find yet another solution (named type-III) for  $\Gamma \geq \Gamma_{II}$  which are different from the type-II and type-I solutions.

Among the three solutions that exist for  $\Gamma_{II} \leq \Gamma \leq \Gamma_I$ , only one will be a true thermodynamically stable solution that describes the system in equilibrium. The solution which is stable can be determined by finding which of the three solutions has the lowest free energy for given  $\Gamma$ . The free energy can be evaluated using the correlation functions calculated within the HNC approximation [13]. Explicitly we calculate the excess (over the ideal gas) free energy  $F^{\text{ex}}$ , or the dimensionless free energy per particle  $f^{\text{ex}} \equiv F^{\text{ex}}/2\pi JN$  with  $N$  being the total number of pancakes in the system as follows: [13]

$$f^{\text{ex}} = \frac{\sigma}{2\Gamma} \sum_n \int d^2\mathbf{r} \left[ -c_n^{(s)}(\mathbf{r}) - w_n^{(s)}(\mathbf{r}) + \frac{1}{2}h_n^2(\mathbf{r}) - h_n(\mathbf{r})c_n(\mathbf{r}) \right] + \frac{1}{2\sigma N_I \Gamma} \sum_q \int \frac{d^2\mathbf{k}}{(2\pi)^2} \left[ -\log(1 + \hat{h}_q(\mathbf{k})) + \hat{h}_q(\mathbf{k}) \right]. \quad (11)$$

Figure 1 shows a typical plot of the free energy as a function of  $\Gamma$  for fixed  $\eta$ . We see that the type-II solutions are everywhere unstable and that  $\Gamma_I$  and  $\Gamma_{II}$  are two spinodal points. We can identify  $\Gamma_c$  where the first order phase transition occurs such that above and below this value the system is described by the type-III and type-I solutions respectively.

It is important to note that this first-order transition is not a melting transition nor does it involve the existence of long-range order in the direction perpendicular to the layers. This can be most easily seen from the structure factor defined by

$$S_n(\mathbf{k}) = 1 + \frac{1}{dN_l} \sum_q \exp(iqnd) \hat{h}_q(\mathbf{k}).$$

Above and below the transition temperature  $\Gamma_c$  the in-plane (*i.e.*  $n = 0$ ) correlation is almost the same as can be seen from the structure factor in  $k$ -space in Fig. 2 (a) and also from the pair correlation function  $h_0(r)$  in real space Fig. 3 (a). We also note that no crystalline long range order exists below the transition, since the peaks have finite widths. The most dramatic changes are observed in the inter-layer correlation. This can be seen by comparing  $S_n(\mathbf{k})$  for  $n \neq 0$  above and below the transition as in Fig. 2 (b)-(d). Compared to the situation above the transition, the system below the transition remains highly correlated even when the layers are far apart. As

one lowers the temperature (increases  $\Gamma$ ) across the transition, the pancake vortices that were more or less independent of those in neighboring layers become instead highly correlated.

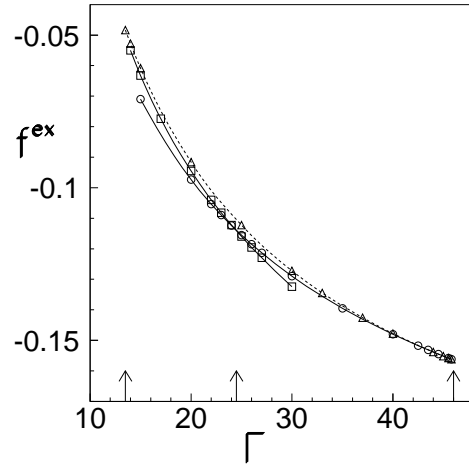


FIG. 1. The excess free energy per pancake  $f^{\text{ex}}$  as a function of  $\Gamma$  for  $\eta = 0.5$ . The free energy for the type-I (circles) and type-III (squares) solutions are shown together with the unstable type-II solutions (triangles, dotted line). The arrow in the middle indicates the transition temperature  $\Gamma_c = 24.5$ . The arrows in the left and right of  $\Gamma_c$  represent the spinodal points  $\Gamma_{II} \simeq 13.0$  and  $\Gamma_I \simeq 49.0$ , respectively.

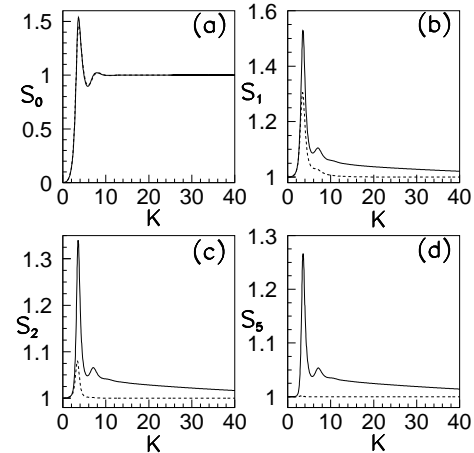


FIG. 2. The structure factor  $S_n(K)$  for (a)  $n = 0$ , (b)  $n = 1$ , (c)  $n = 2$  and (d)  $n = 5$  at  $\eta = 0.5$ , where  $K = ka$  is a dimensionless wavevector. The dotted lines are the type-I solutions at  $\Gamma = 24$  and the solid lines are the type III solutions at  $\Gamma = 25$ .

The phase below the transition described by the type-III solutions is characterized by the tendency there of

the pancake vortices to stack above each other along the field direction. This is clearly demonstrated by the behavior of the pair correlation function  $h_n(\mathbf{r})$ . As can be seen from Fig. 3(c) the type-III solutions for  $h_n(r)$  for  $n \neq 0$  exhibit a singular behavior for small  $r$ . This is in contrast to the type-I solutions shown in Fig. 3(b). The type-I solutions are regular at  $r = 0$ . The singular behavior at small  $r$  in type-III solutions is also reflected in the very slow decay at large  $k$  of the Fourier transformed quantities as seen in Fig. 2(b)-(d). We estimate that  $h_n(r) \sim a_n/r^\alpha$  as  $r \rightarrow 0$  where the constants  $a_n$  and the non-universal exponent  $\alpha$  depend on the temperature parameter  $\Gamma$ . From Eq. (7) we can also deduce that the singularity in  $h_n$  must be cancelled by the same singularity in  $c_n$ , and this is confirmed in our numerical calculation. The singular behavior indicates that below the transition the pancake vortices in different layers have a large probability of being on top of each other and so behave more like stiff vortex lines rather than individual pancake vortices. One way to see the correlation perpendicular to the layers is from the  $n$ -dependence of  $h_n(r)$  for fixed  $r$ . For example for  $r \simeq 0$ , this quantity decreases very rapidly to zero as seen from Fig. 3(b) for the type-I solutions. This shows that the correlation length along the field direction is short. On the other hand, Fig. 3(d) shows that, below the transition,  $h_n(r)$  decays very slowly with  $n$  and appears to approach a non-zero value suggesting that there might even be long-range order present. As will be demonstrated later in this section, this is not the case. In fact there seems to be no order parameter that describes correlation across the layers which becomes non-vanishing below the transition. Thus our transition seems to be best described as a liquid-liquid transition for which the low-temperature phase has much longer correlations along the field direction than the high-temperature phase.

Using the calculated correlation functions, one can also determine other thermodynamic quantities like the excess internal energy  $U^{\text{ex}}$ . The dimensionless internal energy per particle,  $u^{\text{ex}} = U^{\text{ex}}/2\pi JN$  is given by

$$u^{\text{ex}} = \frac{\sigma}{2\Gamma} \sum_n \int d^2\mathbf{r} w_n(\mathbf{r}) h_n(\mathbf{r}).$$

The specific heat per pancake excluding the ideal gas contribution can be calculated by differentiating the internal energy with respect to the temperature:  $c_v = N^{-1}d(U^{\text{ex}}/d\Gamma) = k_B(du^{\text{ex}}/d\Gamma^{-1})$ . The inset of Fig. 4 shows that the specific heat in our system obtained by numerically differentiating  $u^{\text{ex}}$ . The specific heat is larger in the low temperature phase consistent with general features of an ordinary phase transition. The liquid-to-liquid phase transition observed in [2] is quite unusual in the sense that the low temperature phase has a smaller specific heat. We believe this is also a consequence of disorder which in addition to changing the order of the

transition might also modify the sign of the specific heat jump [7].

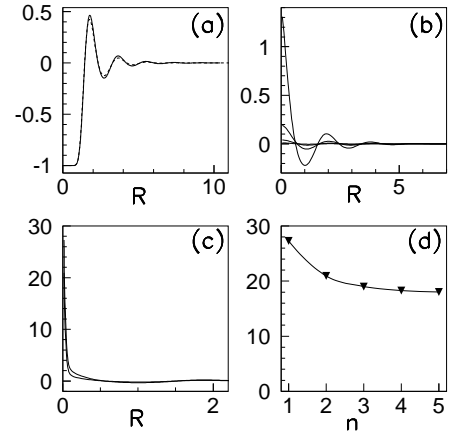


FIG. 3. The pair correlation function  $h_n(R)$  for  $\eta = 0.5$  from the type-I ( $\Gamma = 24$ ) and type-III ( $\Gamma = 25$ ) solutions with dimensionless  $R = r/a$ . (a)  $h_0(R)$  from the type-I (dotted line) and type-III (solid line) solutions; (b) The type-I  $h_n(R)$  for  $n = 1, 2, 3$  and 4. The overall magnitude of  $h_n(r)$  gets smaller for larger  $n$ ; (c) The type-III  $h_n(R)$  for  $n = 1$  and 2. (d) The type-III  $h_n(r_0)$  as a function of  $n$  for very small fixed  $r_0 \simeq 0.016$ .

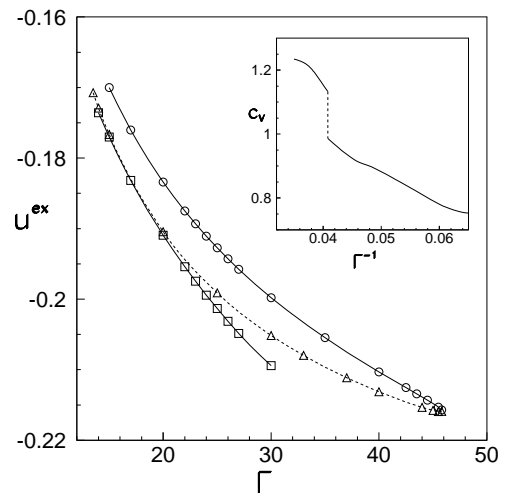


FIG. 4. The excess internal energy  $u^{\text{ex}}$  per pancake as a function of  $\Gamma$ . The type-I (circles), type-II (triangles) and type-III (squares) solutions are shown. The inset is the plot of the specific heat versus temperature  $\Gamma^{-1}$ .

For other values of  $\eta$ , the first-order transition point  $\Gamma_c$  can in principle be determined in the way described above. This will then lead to a transition line in the physical  $B$ - $T$  plane on using Eq. (3). Unfortunately, we

found it quite difficult using our iterative technique to obtain type-III solutions starting from type-II solutions especially when  $\eta$  becomes larger, since they have a very different form from the type-II solutions especially in the small- $r$  region. In the present analysis we were only able to identify a couple of transition points which are shown in Fig. 5. It is, however, relatively easy to find the spinodal points where the type-I and type-II solutions cease to exist. The collection of these points up to very large values  $\eta$  are shown in Fig. 5. If there were a critical point as in an ordinary liquid-gas phase transition, the two spinodal lines would have to meet at the critical point. Fig. 5 shows that the two spinodal lines almost run parallel to each other in the large  $\eta$  region. Therefore within our model the phase transition seems to continue into both the large and small  $\eta$  regime, implying that no critical points exist. We also note that the slope of the phase transition line is opposite to those of the spinodal lines. Since the transition line should lie between two spinodal lines, we expect that as we go to the large- $\eta$  region the transition line will change its direction and show a kind of re-entrant behavior in the  $\eta$ - $\Gamma$  space.

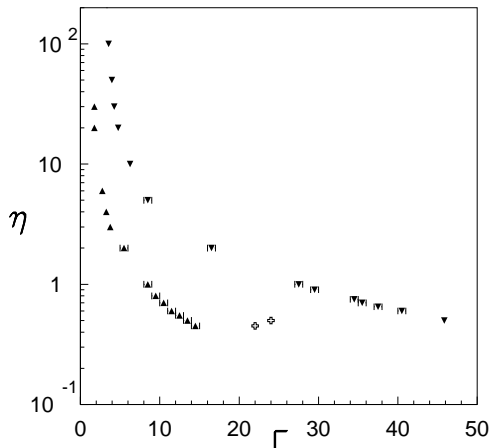


FIG. 5. The spinodal points  $\Gamma_I$  (inverted triangles) and  $\Gamma_{II}$  (triangles). The first-order transition points (crosses) for  $\eta = 0.45$  and  $0.5$ .

The liquid phase described by the type-III solutions is characterized by the inter-layer correlation functions becoming singular at small  $r$  and decaying very slowly with  $n$  (the layer separation) at fixed  $r$ . For a system consisting of  $N_l = 11$  layers, Fig. 3(d) shows the correlation function almost becomes a non-zero constant for large layer separation  $n$ . If this continues to be the case for larger systems, then it would imply that there is indeed long-range order below the transition in the direction perpendicular to the layers. We therefore investigated the  $c$ -axis correlation function as done in Fig. 3(d) but for

larger systems. The  $c$ -axis correlation function shows a similar behavior for larger systems as seen in Fig. 6. However, from Fig. 6 one can also see that in the limit  $N_l \rightarrow \infty$  the correlation function will decay to zero as  $n$  becomes large, implying that there is no long-range order in the thermodynamic limit. This analysis also tells us that in order to study the true thermodynamic behavior of the system, free from finite size effects, we will have to consider a very large number of layers. This will be a very challenging problem numerically.

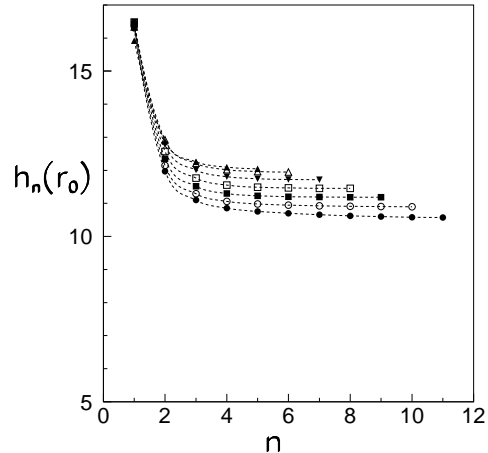


FIG. 6. The pair correlation function  $h_n(r_0)$  for very small fixed  $r_0 \simeq 0.016$  as functions of  $n$ . The two parameters used are  $\Gamma = 17$  and  $\eta = 0.5$ . Systems consisting of  $N_l = 11, 13, \dots, 23$  layers are presented. Because of the periodicity one only has to consider the values of  $n = 1, 2, \dots, (N_l - 1)/2$ .

One aspect which we did not consider in this analysis is the possibility of having crystalline solutions of the HNC equations. In order to study this one has to start from a HNC functional which allows spatial variation of the density. Eventually one has to evaluate and compare the free energies of the crystalline solution with the liquid state solutions. Whether such solutions exist and have a lower free energy than the liquid solution is left for future work. Other possibilities exist such as the crystallization transition (if any) taking place at a lower temperature than the liquid-liquid transition. Evidence of two transitions has actually been seen in a simulation of pancakes interacting with screened interactions [14]. On this scenario one would argue that the presence of disorder removes the crystalline phase at large fields leaving just the liquid-liquid transition. In principle, because different symmetries are involved, a liquid-liquid transition followed by a liquid-crystal transition on further cooling is a distinct possibility, although intuitively one might expect that the temperature interval between the liquid-liquid transition and the onset of crystalliza-

tion might be small. Maybe only the presence of disorder makes the liquid-liquid transition clearly visible as a distinct transition.

In summary we have considered a model for pancake vortices in layered superconductors by deriving a pair potential for them. Using the HNC approximation we have found that there is a first-order transition within the vortex liquid phase without any critical end-points. No long-range order associated with the transition could be identified. However, in the low-temperature phase the pancake vortices stack up to form stiff vortex lines. In order to study the rich phase structure exhibited by high temperature superconductors in a magnetic field it will be necessary to include the effect of disorder into the present analysis. This will change our first order transition into a continuous transition above some critical field [7].

JY was supported by grant No. 1999-2-112-001-5 from the interdisciplinary research program of KOSEF. MAM would like to thank F. Thalmann for many useful discussions.

- 
- [1] W. K. Kwok, J. Fendrich, S. Fleshler, U. Welp, J. Downey, and G. W. Crabtree, *Phys. Rev. Lett.* **72**, 1092 (1994); R. Liang, D. A. Bonn, and W. N. Hardy, *Phys. Rev. Lett.* **76**, 853 (1996); A. Schilling, R. A. Fisher, N. E. Phillips, U. Welp, D. Dasgupta, W. K. Kwok, and G. W. Crabtree, *Nature (London)* **382**, 791 (1996).
- [2] F. Bouquet, C. Marcenat, E. Steep, R. Calemczuk, W. K. Kwok, U. Welp, G. W. Crabtree, R. A. Fisher, N. E. Phillips, and A. Schilling, *Nature (London)* **411**, 448 (2001).
- [3] M. Roulin, A. Junod, A. Erb, and E. Walker, *Phys. Rev. Lett.* **80**, 1722 (1998); A. Schilling, R. A. Fisher, N. E. Phillips, U. Welp, W. K. Kwok, and G. W. Crabtree, *Phys. Rev. Lett.* **78**, 4833 (1997).
- [4] A. A. Zhukov, P. A. J. de Groot, S. Kokkaliaris, E. di Nicolò, A. G. M. Jansen, E. Mossang, G. Martinez, P. Wyder, T. Wolf, H. Küpfer, H. Asaoka, R. Gagnon, and L. Taillefer, *Phys. Rev. Lett.* **87** 017006 (2001).
- [5] A. K. Kienappel and M. A. Moore, *Phys. Rev. B* **60**, 6795 (1999); J. Yeo and M. A. Moore, *Phys. Rev. B* **64**, 024514 (2001).
- [6] M. V. Feigel'man, V. B. Geshkenbein, L. B. Ioffe, and A. I. Larkin, *Phys. Rev. B* **48**, 16441 (1993); Y.-H. Li and S. Teitel, *Phys. Rev. B* **47**, 359 (1993); T. Chen and S. Teitel, *Phys. Rev. B* **55**, 11766 (1997); P. Olsson and S. Teitel, *Phys. Rev. Lett.* **82**, 2183 (1999); A. K. Nguyen and A. Sudbø, *Phys. Rev. B* **58**, 3438 (1998); X. Hu, S. Miyashita and M. Tachiki, *Phys. Rev. Lett.* **79** 3498 (1997).
- [7] Y. Imry and M. Wortis, *Phys. Rev. B* **19**, 3580 (1979); D. Boyanovsky and J. Cardy, *Phys. Rev. B* **25**, 7058 (1982); S. Chen, A. M. Ferrenberg, and D. P. Landau, *Phys. Rev. E* **52**, 1377 (1995).
- [8] J. P. Hansen and I. R. McDonald, *Theory of Simple Liquids*, (Academic Press, London, 1986).
- [9] G. I. Menon and C. Dasgupta, *Phys. Rev. Lett.* **73**, 1023 (1994); P. S. Cornaglia and C. A. Balseiro, *Phys. Rev. B* **61**, 784 (2000).
- [10] W. E. Lawrence and S. Doniach, *Proceedings of the 12th international conference on low temperature physics*, Kyoto, Japan, edited by E. Kanda (Keikaku, Tokyo, 1971)
- [11] J. P. Hansen and D. Levesque, *J. Phys. C* **14**, L603 (1981); J. M. Caillol, D. Levesque, J. J. Weis, and J. P. Hansen, *J. Stat. Phys.* **28**, 325 (1982).
- [12] K.-C Ng, *J. Chem. Phys.* **61**, 2680 (1974).
- [13] T. Morita and K. Hiroike, *Prog. Theo. Phys.* **23**, 1003 (1960); **25**, 537 (1961); M. Mézard and G. Parisi, *J. Chem. Phys.* **111**, 1076 (1999).
- [14] N. K. Wilkin and H. J. Jensen, *Europhysics Letters* **40**, 423 (1997).